Fusion of Angiography and Intravascular Ultrasound In-Vivo: Establishing the Absolute 3-D Frame Orientation

Andreas Wahle,* *Member, IEEE*, Guido P. M. Prause, Clemens von Birgelen, Raimund Erbel, and Milan Sonka, *Member, IEEE*

***Abstract* — Data fusion of biplane angiography and intravascular ultrasound (IVUS) facilitates geometrically correct reconstruction of coronary vessels. The locations of IVUS frames along the catheter pullback trajectory can be identified, however the IVUS image orientations remain ambiguous. An automated approach to determination of correct IVUS image orientation in 3-D space is reported. Analytical calculation of the catheter twist is followed by statistical optimization determining the absolute IVUS image orientation. The fusion method was applied to data acquired in patients undergoing routine coronary intervention, demonstrating the feasibility and good performance of our approach.**

***Index Terms* — Data Fusion, Multimodal 3-D Reconstruction, Biplane Angiography, Intravascular Ultrasound.**

I. Introduction

For the assessment of atherosclerotic disease, two major imaging modalities are commonly utilized. Quantitative Coronary Angiography (QCA) is a well-established standard, for which many semi-automated systems are available [1]–[4]. By using biplane angiography, any spatial structure visible in both projections can be geometrically reconstructed in the 3-D space. Information about the imaging geometry [5]–[7], and the assignment of corresponding vessel segments between both projections are the prerequisites [8], [9]. Recently, intravascular ultrasound (IVUS) evolved as a complementary method; a comprehensive overview of the existing methods for IVUS image acquisition and analysis can be found in [10]. While selective angiography depicts the vessel lumen only, IVUS allows to analyze vascular wall and plaque. However, IVUS lacks a geometrically correct 3-D representation since it provides no information about vessel curvature. Current 3-D IVUS systems reconstruct vessels by straight stacking of the frames [11].

Fusion of IVUS and biplane angiography may yield a geometrically correct assignment of the volume elements into 3-D space, retaining the original relationships between them even in tortuous vessels. Analytical derivation of the curvature using the Frenet-Serret formulas can solve the problem of determining the *relative* orientation changes (*twist*) between adjacent IVUS frames [12]. However, the definition of the *absolute* orientation remains mostly unconsidered. The problem is comparable to fitting a sock on a leg [13]: While the leg (catheter path) is stable, the sock (axial frame orientation) can be freely rotated around the leg, but fits optimally only in one orientation. Current approaches either try to match the IVUS contours with the angiographic profiles by backprojection [14], or rotate the entire set interactively until the images approximately match the angiographic outline [13]. The use of branches as natural landmarks is frequently unreliable since they may be difficult to identify in both the angiograms and IVUS images [15].

This paper focuses on the absolute orientation problem. We are using the bending behavior of the imaging catheter as a reference. The catheter is expected to fall in the position of minimum energy within the vessel (Figs. 1, 2). The out-of-center position of the catheter within the lumen is used as a reference for the determination of the absolute orientation of the IVUS frames. After reconstruction of the catheter path and the cross-sections using an initial orientation, the difference angles between the out-of-center positions derived from the angiograms vs. the IVUS data are compared. The overall error is minimized by applying a corrective axial rotation to all IVUS frames calculated using a statistical approach.

II. Methods

A. 3-D Catheter Path and Vessel Outline

The biplane angiograms used for extraction of the catheter path as well as the outline of the vessel lumen are taken immediately before the IVUS pullback start and are corrected for geometrical distortions in a preprocessing step [15]. Within a specified region of interest, the catheter path is automatically determined from the angiograms by applying a dynamic programming approach [16]. In a second step, the vessel borders are extracted based upon the detected catheter path.

From the known imaging geometry, both the catheter path and the vessel outline are reconstructed using the method previously developed and validated at the German Heart Institute of Berlin [17], [18]. The reconstruction yields a combined 3-D model of the catheter and the vessel lumen, the latter restricted to elliptical cross sectional shapes.

This work has been supported in part by grants Pr 507/1-2 and Wa 1280/1-1 of the Deutsche Forschungsgemeinschaft [German Research Society], Bonn, Germany. *Asterisk indicates corresponding author.*

*A. Wahle and M. Sonka are with the University of Iowa, Department of Electrical and Computer Engineering, Iowa City, IA 52242, USA (e-mail: a.wahle@ieee.org).

G. P. M. Prause was with the University of Iowa, Department of Electrical and Computer Engineering, Iowa City, IA 52242, USA. He is now with the MeVis Institute at the University of Bremen, D-28359 Bremen, Germany.

C. von Birgelen and R. Erbel are with the University Hospital Essen, Medical Clinic, Department of Cardiology, D-45122 Essen, Germany.

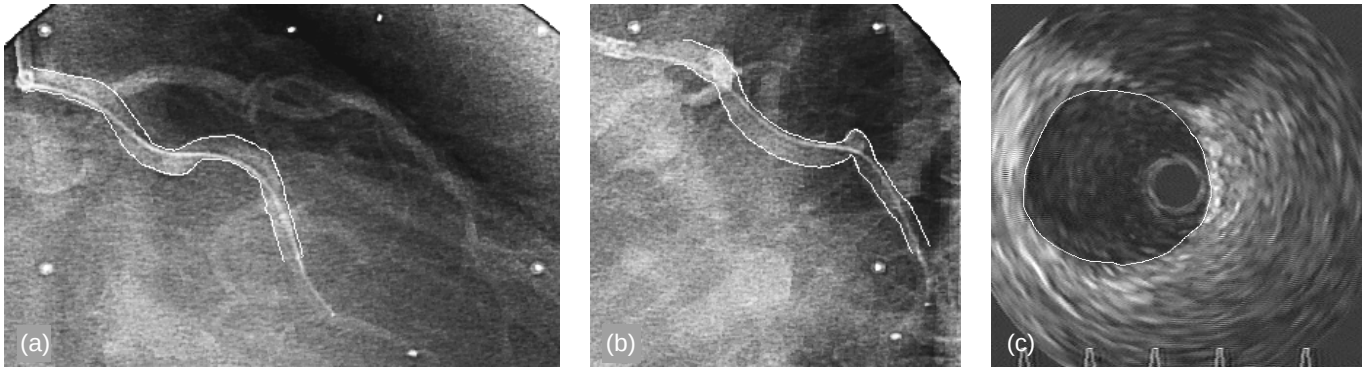

Fig. 1. Angiograms of a circumflex artery in a patient heart using (a) 30° right and (b) 60° left anterior oblique projections, with catheter inserted and the vessel lumen outline detected; (c) automated detection of the lumen border in one of the IVUS images, note the out-of-center position of the catheter.

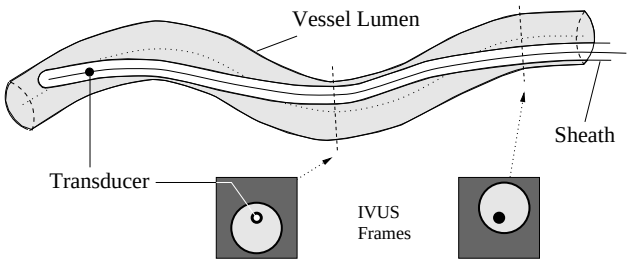

Fig. 2. Bending of the imaging catheter within the vessel due to vessel curvature, seeking position of minimum energy, and associated out-of-center position in IVUS images. While the absolute orientations of the IVUS cross-sections in the images are arbitrary, their orientations relative to each other are fixed.

B. IVUS Frame Location Matching

For a sheathed catheter, the location of the catheter as shown in the angiograms before the catheter pullback start indicates the pullback path of the IVUS transducer, since the sheath remains in its position and only the core is moved (Fig. 2). In-vivo, ECG-gating is mandatory to avoid mismatches due to heart motion. From the time-stamps of a specific frame vs. the frame at the pullback start, along with the known speed of the pullback, the distance of this frame to the start frame on the catheter trajectory can be calculated. The use of a motorized pullback device ensures a sufficiently constant speed of the transducer and consequently a proper matching of the frame positions. The respective 3-D catheter location and the angiographically determined elliptic contour are assigned to their corresponding IVUS frame.

C. Twisting of the IVUS Catheter

The IVUS catheter is twisting whenever the local direction of the pullback trajectory enters a new plane of different spatial orientation. The relative orientation of adjacent IVUS images reflects the catheter twist and can be calculated from the 3-D catheter pullback trajectory using our sequential triangulation method described in [12]. From the orientation of the previous frame and the local path of the catheter, the orientation of the next frame is calculated by a discrete version of the Frenet-Serret formulas. This algorithm has been extensively validated in several in-vitro studies [12], [19].

D. Initial Orientation of the Frame Set

To determine the absolute orientation of the IVUS frame set, the out-of-center positions are derived from the initial frame orientation, which is in theory arbitrary. For reasons of better reproducibility and validation of the catheter twist, the initial orientation is aligned with a reference plane [20]. This reference plane is calculated using bilinear regression from the 3-D catheter trajectory points previously reconstructed from the biplane angiograms (Fig. 3), thus minimizing the distance of the plane to the transducer path. The baseline axis of the first IVUS frame is oriented parallel to this reference plane. The axes of the subsequent IVUS frames are determined with respect to the first frame according to the relative change of orientation as calculated from the relative catheter twist as described above.

E. Calculation of Out-of-Center Vectors

Calculating the out-of-center vectors requires previous (longitudinal) segmentation of the vessel lumen in both angiographic views as well as (cross-sectional) lumen segmentation in all ECG-gated IVUS images of the sequence. Segmentation in angiography is performed as described in subsection A. The IVUS segmentation uses our previously validated semi-automated approach [21].

The longitudinal detection of the angiographic vessel outline in 2-D yields a set of pairs for the left and right edges (*profile*). Since the catheter path is already known, for each IVUS frame location, the 2-D profiles of both angiographic projections are reconstructed to an elliptical contour [17], [18]. From a point within the ellipse in which the catheter path intersects the lumen cross-section, the out-of-center vector is calculated as the vector beginning at the intersection point and ending at the center of the ellipse.

Similarly, the center points are determined for the IVUS frames. This process is more complex since the IVUS-based lumen contour may have a free shape. Assuming a homogeneous distribution of the contour points, which is true for most vessel shapes except in severe stenoses, the centroid for a contour j containing n_j points $[u_{ij}, v_{ij}]$ is calculated by:

$$S_j = [\overline{u}_j, \overline{v}_j] = \frac{1}{n_j} \sum_{i=0}^{n_j-1} [u_{ij}, v_{ij}] \qquad (1)$$

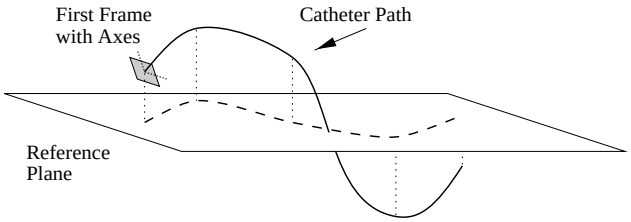

Fig. 3. Reference plane for specification of the initial orientation; the horizontal axis of the first IVUS frame is aligned parallel to the plane.

The location of the catheter within the 2-D image is fixed at the center of the image. Both centroid and catheter points are mapped into the 3-D space by using the image frames reconstructed with the initial orientation. The IVUS out-of-center vector is the vector beginning at the catheter point (image center) and ending at the calculated centroid of the respective IVUS contour.

F. Error Minimization

For each of the IVUS frames, the out-of-center vectors reconstructed from the biplane angiograms are compared with those determined from the IVUS data. In agreement with the image acquisition geometry, the IVUS frames are expected to be oriented perpendicular to the catheter path. The ellipses reconstructed from the angiograms are orthogonal to the vessel centerline, which may differ from the orientations of the IVUS frames. Thus, they have to be projected onto their corresponding frames. Afterwards, the errors (magnitude μ and difference angle φ, Fig. 4) are determined for each frame.

The process of determining the absolute orientation of the IVUS pullback image set is using statistical optimization incorporating several weighting mechanisms. The goal is to minimize the angular difference between the out-of-center vectors derived from the angiographic and the IVUS data. There are several local inaccuracies originating from the reconstruction process, such as limited resolution, slight mismatches in IVUS localization, etc., that may affect the error minimization [19], [20]. To maximize the influence of the reliably measured parameters and minimize the influence of possible inaccuracies, data reliability weight is used in addition to the error measure strength. This is performed by analyzing the data within a moving window of an empirically determined fixed size along the catheter path.

Within the window, each difference angle φ is weighted by the vector length μ, thus giving more weight to larger out-of-center catheter positions (Fig. 4). Obviously, minimizing a rotational error for a catheter close to a wall is more robust than minimizing an error for an almost-centered catheter. Due to the higher resolution, the mapped out-of-center vectors from the IVUS images are used to determine the weight. For each window k, the weighted mean $\overline{\varphi}_k$ and the weighted standard deviation $\sigma(\varphi_k)$ of the difference angles as well as the sum of weights $\Sigma\mu_k$ are calculated. After determination of those three parameters at all locations of the moving window, the correction angle is calculated as a weighted mean of all $\overline{\varphi}_k$. The reliability weight increases with the value of $\Sigma\mu_k$, while it is limited by the local tolerances $\sigma(\varphi_k)$. The final correction

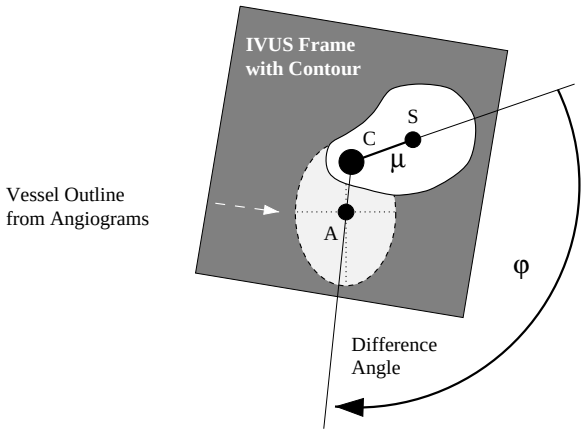

Fig. 4. Determination of the error angle from the out-of-center vectors; the out-of-center strength μ is calculated as the distance from the centroid S to the catheter location C; the error angle φ is enclosed by CS and CA, where A is the center of the angiographically reconstructed ellipse.

angle $\overline{\varphi}_{\mathrm{corr}}$ results from the weighted means:

$$\overline{\varphi}_{\mathrm{corr}} = \sum_k \left(\overline{\varphi}_k \frac{\Sigma\mu_k}{\sigma(\varphi_k)} \right) \Bigg/ \sum_k \left(\frac{\Sigma\mu_k}{\sigma(\varphi_k)} \right) \qquad (2)$$

and is then applied to all IVUS frames.

G. Data Analysis

The information about the 3-D reconstructed vessel can be used for geometrically correct visualization as a VRML-2.0 (Virtual Reality Modeling Language) model (Fig. 5). This model provides excellent visualization of the overall geometry. However, the complete information delivered by IVUS is difficult to assess in this way. Thus, the geometrically correctly positioned IVUS pixel data in 3-D were mapped into a voxel cube of a configurable size. The voxel cube can be arbitrarily sliced to represent visualization at a specific projection angle, and thus allows a direct comparison with angiographic images. If independently acquired angiograms are used, such comparisons may be used for validation purposes (Fig. 6).

III. Results

The catheter twist calculation and the 3-D reconstruction accuracy of the catheter trajectory were previously validated in phantoms and excised pig hearts [12], [19]. No in-vivo validation was performed until now. The results presented below demonstrate the in-vivo feasibility of the developed approach. Three patients with stable coronary artery disease undergoing coronary revascularization and stent placement in native coronary arteries were imaged as part of their clinical procedure. The developed data fusion method was applied to vascular segments of interest in the left anterior descending, left circumflex, and right coronary arteries with 40, 64, and 77 mm in length, respectively. The angiograms were acquired at a biplane Siemens HICOR cath-lab with DICOM output on CD-R. IVUS imaging was performed after advancing the transducer 5 mm past the target segment into the distal vessel. The IVUS images were obtained using sheathed 2.9 F and 3.2 F 30 MHz catheters

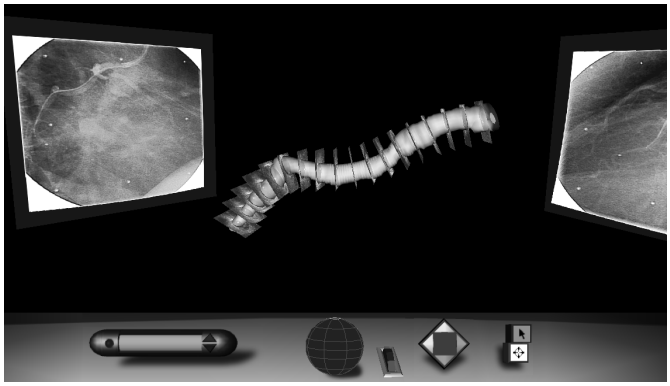

Fig. 5. Interactive VRML visualization of the geometrically correct reconstructed vessel of interest. The vessel geometry is determined from biplane angiography, the vessel lumen was segmented from IVUS images some of them being shown correctly positioned and oriented.

(Boston Scientific, San Jose, CA). The motorized pullback device was activated for 8 s (4 mm, speed 0.5 mm/s) to straighten the catheter core within the vessel. Two pairs of biplane angiograms were acquired in different angulations with the IVUS catheter inserted in the distal location. One of the angiographic pairs was used in the data fusion, the other pair was used for validation. Since no reliable independent standard exists for patients, only limited quantitative validation was possible in-vivo and results were mainly assessed qualitatively.

In all three analyzed in-vivo cases, the reported data fusion approach successfully determined the geometrically correct coronary vessel representation. For the data sets, VRML scenes were created (Fig. 5), 3-D data cubes were constructed and reprojected at angles corresponding to the second pair of biplane angiograms which were not used for data fusion (Fig. 6). The 2-D data were quantitatively analyzed to approximate the IVUS reconstruction accuracy by comparison of the final result with the initial orientation of the IVUS frames. Fig. 6 shows the reconstructed 3-D cube and the functions for μ and φ, as well as the total reliability weight for the artery presented in Fig. 1. For this vessel, the analysis of the 2-D projections in frontal angulation showed a centerline mismatch in object level of 0.73 ± 0.35 mm (max. 1.5 mm) after establishing the absolute orientation, compared with 1.91 ± 0.90 mm (max. 3.6 mm) in the initial orientation.

IV. Discussion

The presented algorithm delivered the true frame orientation in all cases. In contrast to other methods [13], [14], it does not rely on an iterative matching of the angiographic 2-D outlines and projections from the IVUS contours. Instead, it uses an initial IVUS frame orientation to directly calculate a correction angle in 3-D, resulting in the assessment of the optimal orientation in a single step without user interaction.

Vessel segments considered 'reliable' were successfully detected even in cases of poor angiographic visibility of the vessel outline, and vessel segments categorized 'distorted' were automatically discarded. Fig. 6 illustrates the weighting mechanism; the distal part (0–30 mm) consists of an increasing out-of-center position μ (curve d), while the difference angle φ (e) has a relatively high variance. Consequently, only a few windows could earn a high weight (f). Especially around the 25 mm location, where the left anterior oblique angiogram was highly foreshortened, the reliability weight is minimized. The proximal part of the vessel showed higher stability in the angle function φ along with some peaks in the out-of-center position μ (e.g. at 46 mm). Thus, the corresponding values at these locations of the moving window were higher weighted.

In stenosed vessels, irregular shapes (i.e. inaccurate fitting of the ellipse) may cause a large variance in the angle function. Furthermore, if the out-of-center position is less than angiographic resolution (0.5 mm), the angle function is highly distorted as well. Our algorithm ensures that those segments are discarded. However, the existence of at least one 'reliable' segment that exceeds the width of the moving window is necessary for the successful application of our method.

In previous in-vitro studies, we encountered effects that cause a linear rotational phase shift in the IVUS images, presumptively due to friction of the imaging core against the sheath in high curvature [19]. Solid-state catheters could avoid this problem, but are usually not sheathed and cannot provide a stable pullback path as required by our method. Friction effects are mostly additive and thus monotonic, and show some systematics in the angle function. Consequently, the presented approach provides a good basis for detecting and correcting distortions introduced by the imaging system, resulting in a correction function over the pullback length rather than in a single value.

Along with our previously developed and validated methods for geometrical 3-D reconstruction from biplane angiograms, border segmentation from intravascular ultrasound, and analytical calculation of the catheter twist, the presented method has a high potential to overcome a major problem in the reliable determination of the absolute orientations of the IVUS frames. Using the catheter itself as an artificial landmark avoids the need for detecting frequently unreliable anatomic landmarks like vessel branches, or the application of artificial landmarks on the vessel itself.

V. Conclusions

A novel method for determination of the absolute orientation of the IVUS pullback image data was developed and incorporated in our data fusion approach for geometrically correct reconstruction of coronary vessels. The first employment of this complex but nevertheless highly automated data fusion approach in human patients in-vivo was reported. The developed system is able to deliver a high quality reconstruction of the IVUS data, and allows geometrically correct analyses of the vessel, which substantially improves the clinical applicability of both involved modalities.

References

[1] R. L. Kirkeeide, P. Fung, R. W. Smalling, and K. L. Gould, "Automated evaluation of vessel diameter from arteriograms," in *Proc. Computers in Cardiology 1982, Seattle WA*, Los Alamitos CA, pp. 215–218, IEEE-CS Press, 1982.

[2] J. Beier, H. Oswald, H. U. Sauer, and E. Fleck, "Accuracy of measurement in quantitative coronary angiography (QCA)," in *Computer Assisted Radiology (CAR '91)*, H. U. Lemke *et al.*, eds., Berlin/New York, pp. 721–726, Springer, 1991.

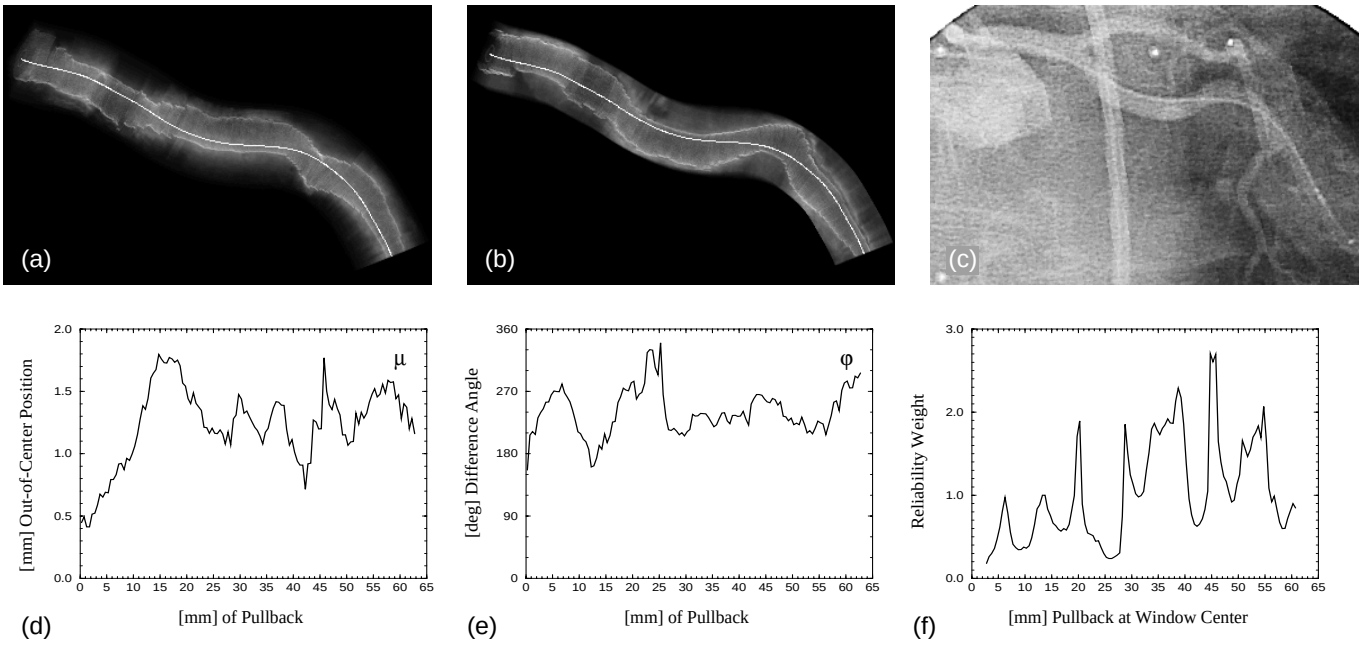

Fig. 6. Frontal projection through the voxel cube with catheter centerline and detected plaque borders previously marked in the 2-D IVUS images; (a) in initial orientation of the frames; (b) after application of the absolute orientation algorithm; (c) independent angiogram in frontal projection for comparison; (d) length μ of the out-of-center vector for each IVUS image; (e) local correction angle φ determined from initial orientation; (f) resulting weighting function $\Sigma\mu_k/\sigma(\varphi_k)$ of the correction angles with a window width of 5 mm. Side branches were not included in the segmentation process, thus the vessel is modeled as a tube.

[3] P. M. J. van der Zwet and J. H. C. Reiber, "A new approach for the quantification of complex lesion morphology: The gradient field transform; basic principles and validation results," *Journal of the American College of Cardiology*, vol. 24, no. 1, pp. 216–224, July 1994.

[4] M. Sonka, M. D. Winniford, and S. M. Collins, "Robust simultaneous detection of coronary borders in complex images," *IEEE Transactions on Medical Imaging*, vol. 14, no. 1, pp. 151–161, Mar. 1995.

[5] H. Wollschläger, P. Lee, A. Zeiher, U. Solzbach, T. Bonzel, and H. Just, "Mathematical tools for spatial computations with biplane isocentric X-ray equipment," *Biomedizinische Technik*, vol. 31, no. 5, pp. 101–106, May 1986.

[6] L. E. Fencil and C. E. Metz, "Propagation and reduction of error in three-dimensional structure determined from biplane views of unknown orientation," *Medical Physics*, vol. 17, no. 6, pp. 951–961, Nov./Dec. 1990.

[7] S. Y. J. Chen, K. R. Hoffmann, and J. D. Carroll, "Three-dimensional reconstruction of coronary arterial tree based on biplane angiograms," in *Medical Imaging 1996: Image Processing*, M. H. Loew and K. M. Hanson, eds., vol. 2710, Bellingham WA, pp. 103–114, SPIE, 1996.

[8] D. L. Parker, D. L. Pope, R. E. van Bree, and H. W. Marshall, "Three-dimensional reconstruction of moving arterial beds from digital subtraction angiography," *Computers and Biomedical Research*, vol. 20, no. 2, pp. 166–185, Apr. 1987.

[9] P. M. Hall, M. Ngan, and P. M. Andreae, "Reconstruction of vascular networks using three-dimensional models," *IEEE Transactions on Medical Imaging*, vol. 16, no. 6, pp. 919–929, Dec. 1997.

[10] J. Dijkstra, A. Wahle, G. Koning, J. H. C. Reiber, and M. Sonka, "Quantitative coronary ultrasound: State of the art," in *What's New in Cardiovascular Imaging?*, J. H. C. Reiber and E. E. van der Wall, eds., Dordrecht, pp. 79–94, Kluwer, 1998.

[11] C. von Birgelen, E. A. de Vrey, G. S. Mintz, A. Nicosia, N. Bruining, W. Li, C. J. Slager, J. R. T. C. Roelandt, P. W. Serruys, and P. J. de Feyter, "ECG-gated three-dimensional intravascular ultrasound: Feasibility and reproducibility of the automated analysis of coronary lumen and atherosclerotic plaque dimensions in humans," *Circulation*, vol. 96, no. 9, pp. 2944–2952, Nov. 1997.

[12] G. P. M. Prause, S. C. DeJong, C. R. McKay, and M. Sonka, "Towards a geometrically correct 3-D reconstruction of tortuous coronary arteries based on biplane angiography and intravascular ultrasound," *International Journal of Cardiac Imaging*, vol. 13, no. 6, pp. 451–462, Dec. 1997.

[13] M. Laban, J. A. Oomen, C. J. Slager, J. J. Wentzel, R. Krams, J. C. H. Schuurbiers, A. den Boer, C. von Birgelen, P. W. Serruys, and P. J. de Feyter, "ANGUS: A new approach to three-dimensional reconstruction of coronary vessels by combined use of angiography and intravascular ultrasound," in *Proc. Computers in Cardiology 1995, Vienna AT*, Piscataway NJ, pp. 325–328, IEEE Press, 1995.

[14] R. Shekhar, R. M. Cothren, D. G. Vince, and J. F. Cornhill, "Fusion of intravascular ultrasound and biplane angiography for three-dimensional reconstruction of coronary arteries," in *Proc. Computers in Cardiology 1996, Indianapolis IN*, Piscataway NJ, pp. 5–8, IEEE Press, 1996.

[15] G. P. M. Prause, S. C. DeJong, C. R. McKay, and M. Sonka, "Semi-automated segmentation and 3-D reconstruction of coronary trees: Biplane angiography and intravascular ultrasound data fusion," in *Medical Imaging 1996: Physiology and Function from Multidimensional Images*, E. A. Hoffman, ed., vol. 2709, Bellingham WA, pp. 82–92, SPIE, 1996.

[16] M. Sonka, V. Hlavac, and R. Boyle, *Image Processing, Analysis, and Machine Vision*. Pacific Grove: PWS Publishing, 2nd ed., 1998/99.

[17] A. Wahle, E. Wellnhofer, I. Mugaragu, H. U. Sauer, H. Oswald, and E. Fleck, "Assessment of diffuse coronary artery disease by quantitative analysis of coronary morphology based upon 3-D reconstruction from biplane angiograms," *IEEE Transactions on Medical Imaging*, vol. 14, no. 2, pp. 230–241, June 1995.

[18] A. Wahle, *Präzise dreidimensionale Rekonstruktion von Gefäßsystemen aus biplanen angiographischen Projektionen und deren klinische Anwendung*. No. 152 in Fortschritt-Berichte, Reihe Biotechnik (17), Düsseldorf: VDI Verlag, 1997. (in German).

[19] A. Wahle, G. P. M. Prause, S. C. DeJong, and M. Sonka, "3-D fusion of biplane angiography and intravascular ultrasound for accurate visualization and volumetry," in *Medical Image Computing and Computer-Assisted Intervention (MICCAI '98)*, W. M. Wells *et al.*, eds., Berlin/New York, pp. 146–155, Springer, 1998.

[20] A. Wahle, G. P. M. Prause, S. C. DeJong, and M. Sonka, "Accurate 3-D fusion of angiographic and intravascular ultrasound data," in *Computer Assisted Radiology and Surgery (CAR '98)*, H. U. Lemke *et al.*, eds., Amsterdam, pp. 164–169, Elsevier, 1998.

[21] M. Sonka, X. Zhang, M. Siebes, M. S. Bissing, S. C. DeJong, S. M. Collins, and C. R. McKay, "Segmentation of intravascular ultrasound images: A knowledge-based approach," *IEEE Transactions on Medical Imaging*, vol. 14, no. 4, pp. 719–732, Dec. 1995.